Well-Ordered Polymer Melts with 5 nm Lamellar Domains from Blends of a Disordered Block Copolymer and a Selectively Associating Homopolymer of Low or High Molar Mass

Vijay R. Tirumala,[†,‡] Vikram Daga,[†] August W. Bosse,[‡] Alvin Romang,[†] Jan Ilavsky,[§] Eric K. Lin,[‡] and James J. Watkins*[,†]

Polymer Science and Engineering, University of Massachusetts, Amherst, Massachusetts 01003; Polymers Division, National Institute of Standards and Technology, Gaithersburg, Maryland 20899; and Advanced Photon Source, Argonne National Laboratory, Argonne, Illinois 60559

Received May 20, 2008; Revised Manuscript Received August 25, 2008

ABSTRACT: The use of short chain block copolymer melts as nanostructured templates with sub-10 nm domains is often limited by their low segregation strength (χN). Since increasing molar mass to strengthen segregation also increases the interdomain spacing of block copolymer melts, it is more desirable to increase the Flory−Huggins segment−segment interaction parameter, χ, to produce strong segregation. We have recently shown that poly(oxyethylene−oxypropylene−oxyethylene) block copolymer melts can undergo disorder-to-order transition when blended with a selectively associating homopolymer that can hydrogen bond with one of the blocks. Here, we study the effect of the molar mass of poly(acrylic acid) in the range 1−13 times that of the copolymer on the segregation of a 6.5 kg/mol poly(oxyethylene−oxypropylene−oxyethylene) copolymer melt. The neat copolymer is disordered, and the addition of poly(acrylic acid) resulted in a well-ordered lamellar morphology with an interdomain spacing of 10 ± 1.0 nm. Using small-angle and ultrasmall-angle X-ray scattering, we found that the blends remain well ordered at 80 °C over the entire range of homopolymer chain lengths. A small increase in the interdomain spacing of the lamellae and an order−order transition from lamellae-to-cylindrical morphology was observed in all blends as a function of increasing homopolymer concentration. The trends observed in experiments were validated by self-consistent field theoretical simulations.

Introduction

Block copolymers are increasingly used in a variety of applications as nanostructured materials for phase-selective materials processing.[1−10] More recently, microphase-separated block copolymers have emerged as promising candidates for next-generation lithographic and pattern-transfer applications in the semiconductor industry.[11−16] However, the sub-10 nm features required in such applications are often limited by the interdomain spacing of microphase-separated block copolymer segments which is proportional to the copolymer molar mass. The small interdomain spacing required in such applications thus necessitates the use of low molar mass block copolymers, often with a molar mass less than 10 kg/mol.

The segregation strength of block copolymers, which represents their propensity for microphase separation, is given by the product of a segment−segment interaction parameter (χ) and the number of monomer units on the copolymer chain (N).[17,18] Consequently, low molar mass block copolymers cannot undergo microphase separation unless χ is large enough to compensate for their limited N. While designing low molar mass block copolymers synthesized from a prescreened pair of polymers with a large χ is one way to circumvent this problem, it is more desirable to explore avenues that increase the effective copolymer segregation strength through an additive. The effect of a homopolymer (macromolecular additive) on the phase behavior of a block copolymer depends subtly on a number of factors such as the segregation strength χN and composition f of the copolymer, the molar mass of homopolymer relative to that of the copolymer (α), and the volume fraction of homopolymer in the blend (ϕ).[19−24] In general, the addition of a homopolymer that is chemically identical to one of the copolymer segments was shown to decrease the segregation strength of strongly segregated symmetric block copolymer melts.[25−29] The selective solubilization of a homopolymer A in a symmetric diblock copolymer AB also increases the lamellar interdomain spacing by as much as 100% at a blend composition of 50% homopolymer by volume.[20,27,30] On the other hand, it has been shown that the order−disorder transition (ODT) temperature of block copolymers can be tuned by the addition of a small-molecule that selectively associates with one of the copolymer segments.[31−35] For example, Epps et al. reported as much as 70 °C increase in the ODT temperature of poly(styrene−isoprene−oxyethylene) triblock copolymers with the addition of lithium perchlorate, a small molecule which is selectively miscible with poly(oxyethylene) segments.[35]

One difference between polymeric and small-molecule additives on segregation in block copolymers with moderate molar mass (≥20 kg/mol) is the large entropic gain associated with mixing the latter with the copolymer segments. However, this difference should be indistinguishable when the homopolymer additive is of sufficiently low molar mass. We have recently found that the addition of a low molar mass (generally less than 10 kg/mol) homopolymer, which selectively associates with one of the copolymer segments via hydrogen bonding, substantially increases the segregation strength of low molar mass amphiphilic triblock copolymer melts.[36] More specifically, we have shown that the addition of low molar mass poly(acrylic acid) (PAA; $M_n \approx 2$ kg/mol) to a sphere-forming, low molar mass (≈8.5 kg/mol) poly(oxyethylene−perdeuterated oxypropylene−oxyethylene) triblock copolymer melt increases the order−disorder transition temperature by as much as 150 °C. To the best of our knowledge, this was the first report of induced order in a disordered low molar mass block copolymer with the addition of a homopolymer.

* Corresponding author. E-mail: watkins@polysci.umass.edu.
† University of Massachusetts.
‡ National Institute of Standards and Technology.
§ Argonne National Laboratory.

10.1021/ma801124n CCC: $40.75
Published on Web 10/16/2008

Here, we address the effect of homopolymer molar mass on the strength of phase segregation in symmetric poly(oxyethylene−oxypropylene−oxyethylene) triblock copolymer/PAA blends and draw two important conclusions. First, we show that in the range of 2−88 kg/mol the molar mass of homopolymer has little effect on the disorder-to-order transition (DOT) achieved by selective association via hydrogen bonding or the lamellar interdomain spacing, which indicates that the system is robust enough to sustain large disparities in the molar mass of components. Second, we report that the addition of the small-molecule analogue of PAA repeat unit, 1-propanoic acid, does not induce order in the disordered copolymer melt, which indicates that these results cannot be directly compared to the studies of selectively associating supramolecular additives.

An understanding of the blend thermodynamics is necessary to predict the rich phase space of ternary systems. The phase behavior of block copolymer (A−B)/homopolymer (C) blend system is governed by the complex interplay between the three segment−segment Flory−Huggins interaction parameters, χ_{AB}, χ_{AC}, and χ_{BC}.[37] The addition of a selectively *miscible but noninteracting* C (defined by the condition $\chi_{AC} = 0$; $\chi_{BC} \approx \chi_{AB}$) increases the effective volume fraction, f_A, of the miscible segments but does not affect either χ_{AB} or N. Mean field theoretical calculations show that the increase in f_A changes the quench depth of the blend relative to that of the neat copolymer, which affects the blend morphology. If C *selectively associates* with A ($\chi_{AC} < 0 < \chi_{AB}$), however, the addition of homopolymer would simultaneously affect the effective quench depth of the blend ($(\chi N)_{AB} - (\chi N)_{AB,spinodal}$) and the effective volume fraction of the miscible segments ($\phi_{eff} \approx \phi_{A+C}$). In such a case, the system traverses the thermodynamic χN vs ϕ phase space at an acute angle with the addition of a selectively associating homopolymer.

As a first step to establish the key thermodynamic parameters that govern this complex phenomenon, we systematically studied the effect of homopolymer molar mass on the morphological phase behavior of commercially available symmetric poly(oxyethylene−oxypropylene−oxyethylene) (Pluronic P105; nominally, PEO_{37}−PPO_{56}−PEO_{37}) triblock copolymer with an average molar mass of 6.5 kg/mol. Pluronic P105 has PEO and PPO in equal volume fractions and should thus form lamellar morphology in the ordered state. However, the low molar mass of Pluronic P105 ($N \approx 158$) together with the small PEO−PPO interaction parameter ($\chi_{PEO-PPO} \approx 0.079$ at 80 °C) results in a segregation strength of 12.5 in the melt state above 65 °C. This value is well below the mean-field segregation strength required for microphase separation of ABA triblock copolymers (≈ 19.5) and indicates that Pluronic P105 remains highly phase mixed in the melt state. The situation is further complicated by the presence of PEO−PPO diblock copolymer as an impurity in the moderately polydisperse Pluronic P105 (PDI $\approx$ 1.27). The nanoscale morphologies of Pluronic P105/PAA blends were studied in the melt state at 80 °C using small-angle X-ray scattering (SAXS). Ultrasmall-angle X-ray scattering (USAXS) was additionally used to probe the possibility of homopolymer macrophase separation into droplets of micrometer or larger length scales.

The physics behind the problem of mixing a selectively associating homopolymer C to AB diblock copolymer was treated recently using a phenomenological model by ten Brinke and co-workers.[38,39] Assuming that the system is in the strong segregation limit, this model can be used to predict the scaling of interdomain spacing with the addition of a homopolymer. While the predictions from this simple calculation for scaling of interdomain spacing with the addition of homopolymer qualitatively agree with our experimental results for lamellar phase, the model is strictly applicable to a limited phase space and does not account for varying homopolymer molar mass. To address this limitation with respect to the system in this study, we performed self-consistent field theoretical (SCFT) calculations to determine whether the addition of a homopolymer with modest selective interactions induces a disorder-to-order transition in weakly segregated, symmetric ABA triblock copolymers. The results from SCFT simulations were then used to extract the scaling of interdomain spacing as a function of the added homopolymer volume fraction and degree of polymerization for comparison with experimental data.

Table 1. Molecular Characteristics of the Systems Used in This Study

sample	M_n (g/mol)	polydispersity index	equivalent EO units[a] (N_{EO})	ideal, unperturbed R_g (nm)[b]
Pluronic P105	6500	1.27	157	
PAA-8	8500	1.07	218.5	4.44
PAA-20	20000	1.09	500	6.8
PAA-44	44000	1.08	1100	10.1
PAA-88	88000	1.12	2200	14.3
AA	72	1		

[a] The molar volumes of EO, PO, and AA monomers were taken as 37.5, 55.5, and 67.5 cm^3, respectively. For example, the chain length of PAA-8 in equivalent units was calculated as $N_{PAA-8} \approx (8500/72) \cdot (67.5/37.5) \cdot N_{EO}$. [b] The ideal, unperturbed radius of gyration (R_g) for PAA homopolymer is calculated from statistics of Gaussian chain, $R_g \approx b(N_{PAA}/6)^{1/2}$ and by assuming b to be on the order of 1 nm.

Materials and Methods

Materials. Commercially available Pluronic P105 copolymer ($PEO_{37}PPO_{54}PEO_{37}$) was generously donated by BASF and was used as-received without further purification.[40] Poly(acrylic acid) (PAA) homopolymer of four different molar masses was obtained from Polymer Source, Inc. The homopolymer was synthesized by the anionic polymerization of *tert*-butyl acrylate followed by the hydrolysis of the ester group. The molecular parameters of the block copolymer and homopolymers used in this study are determined from gel permeation chromatography and are listed in Table 1. The molar masses of PAA were chosen such that they span a range of 1.4−13 times that of the Pluronic P105 copolymer. Considering that the molecular volume of AA monomer is 1.85 times that of the EO monomer unit, this range of PAA molar masses translates into a range of approximately 220−2200 for PAA chain length, N_{PAA}, in the number of EO units.

Sample Preparation. Blend samples of Pluronic P105 copolymer and PAA were prepared by dissolving them at a given mass ratio in anhydrous ethanol. Bulk samples of about ~1 mm thickness were cast from solution and were annealed at 80 °C under vacuum for 24 h. The samples were encapsulated between Kapton windows of $\approx$25 μm thickness.

Small-Angle X-ray Scattering. Small-angle X-ray scattering (SAXS) experiments were performed using the Rigaku-Molecular Metrology SAXS equipment at W.M. Keck Nanostructures Laboratory at University of Massachusetts−Amherst. Samples were measured at 80 °C under vacuum after equilibrating them for at least 3 h at the measurement temperature. Scattered X-rays were collected onto a 2-D wire array detector located at a distance of 1.195 m, which corresponds to a measured q range of 0.006 $Å^{-1} < q < 0.16$ $Å^{-1}$, where $q = (4\pi/\lambda)\sin(\theta)$ and 2θ is the angle over which scattering data are collected. The raw scattering data from each sample were azimuthally averaged and presented in arbitrary intensity units without further corrections.

Ultrasmall-Angle X-ray Scattering. Ultrasmall-angle X-ray scattering (USAXS) measurements were performed at beamline 32-ID-B of the Advanced Photon Source at Argonne National Laboratory.[41] The incident X-ray beam, defined by a rectangular slit to be 2 mm wide × 1 mm tall, with 11.9 keV energy and a flux of (1.0−1.3) × 10^{11} photons/s was used to probe the large-scale structure of blend samples. The scattering data were collected using a point detector and were processed following previously established

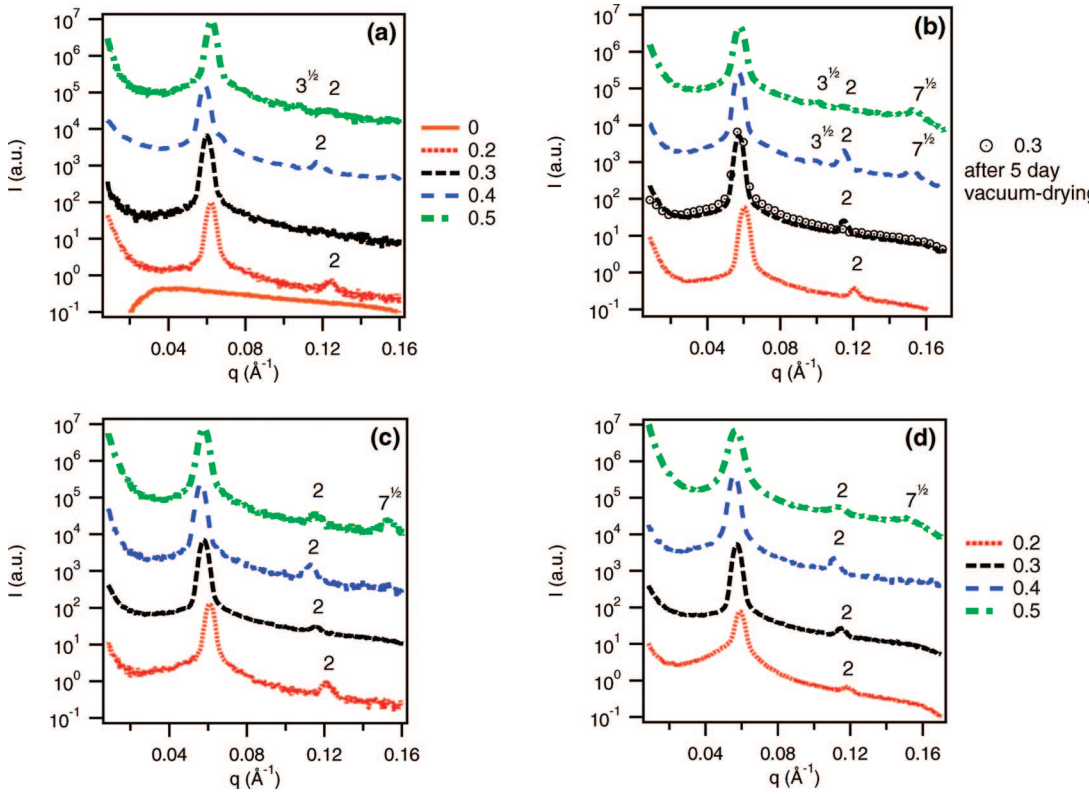

Figure 1. Small-angle X-ray scattering spectra from Pluronic P105 copolymer blended with PAA of molar masses (a) 8.5, (b) 20, (c) 44, and (d) 88 kg/mol as a function of homopolymer mass fraction in the blend measured at 80 °C.

procedures.[42] An empty cell with two Kapton windows was used for background subtraction. The data are presented in a slit-smeared mode since desmearing of a Bragg peak is more involved and is not pertinent to the current study.

Simulation Methods. The triblock copolymer ABA/homopolymer C blend was simulated on a square 256 × 256 periodic lattice using a variation of the real space framework pioneered by Drolet and Fredrickson and the pseudospectral numerical method introduced by Rasmussen and co-workers.[43−47] This solution method requires no a priori knowledge about the symmetry of resulting polymer phase morphology, allowing for reasonable unbiased relaxation toward an energy minimum. Here we provide definitions of the parameters relevant to our simulations. The canonical SCFT utilized in this study is based on a continuous bead−spring model of an incompressible melt of n ABA triblock copolymers and n_h C homopolymers in a volume, V.[44] The index of polymerization for the copolymer is given by N, and the index of polymerization for the homopolymer is given by $N_h \equiv \alpha N$, where α is the homopolymer degree of polymerization relative to that of the copolymer. The average total volume fraction of the C segments is given by $\phi_c = n_h\alpha N/(nN + n_h\alpha N)$. The lattice spacing is set to $\Delta x = \Delta y = 0.25R_g$, where R_g is the copolymer radius of gyration. The values of α and ϕ_c were varied in the range 0.25−8 and 0.1−0.5, respectively, for the simulations discussed here. Segment−segment interactions are parametrized by the traditional Flory−Huggins χ parameters. For the ABA/C blend system of interest here, there are three independent parameters, χ_{AB}, χ_{BC}, and χ_{AC}. The ABA copolymer is assumed to be symmetric so that the total fraction of A segments along the chain is given by f and the copolymer composition is given by $A_{f/2}B_{(1-f)}A_{f/2}$.

The numerous segment−segment interactions that complicate this model are decoupled to yield a formally equivalent polymer field theory, expressed in terms of a single ABA copolymer and a single C homopolymer interacting with three external fields.[45] Mean-field solutions are then obtained by "self-consistently" minimizing the theory's energy functional with respect to the three fields (the so-called "saddle point approximation"). Standard observables, such as the local volume fractions of A segments ϕ_A, B segments ϕ_B, and C segments ϕ_C, are calculated as functional derivates of the energy functional.[45]

All simulations were started from random initial conditions and run for 20 000 complete self-consistent iterations (subsequently referred to as *time steps*). This number of time steps allowed for sufficient relaxation of the system to determine whether the blend was microphase-separated, homogeneous, or macrophase-separated and for an accurate measurement of the microphase domain spacing using Fourier space methods (as discussed below).

Results

Small-Angle X-ray Scattering. Figures 1a−d show the small-angle X-ray scattering intensity measured as a function of scattering wave vector (q) at 80 °C for Pluronic P105/PAA blends of homopolymer composition and molar mass in the range 0−0.5 and 8.5−88 kg/mol, respectively.[48] The X-ray scattering intensity from neat Pluronic P105 copolymer melt decreases with q as should be the case for a low molar mass block copolymer melt in a disordered state well above the ODT temperature (Figure 1a). This is unlike the weak scattering peak (corresponding to "correlation hole") observed typically for block copolymers of high molar mass in a disordered state. The absence of such a correlation peak in scattering from disordered Pluronic copolymer melts may be attributed to the weak PEO−PPO segregation strength, low molar mass, and their polydispersity.

The addition of PAA-8 to Pluronic P105 at 20% by mass results in a significantly correlated scattering intensity with a relatively sharp scattering peak at $q^* \approx 0.0625 \pm 0.006$ Å^{-1}. In addition, there exists a secondary scattering peak at $q \approx 0.125$ Å^{-1}, and the ratio of wave vectors associated with the primary and secondary scattering peaks is 1:2, which corresponds to a relatively well-ordered lamellar morphology with a domain spacing of ∼10.05 nm. The secondary scattering peak disappeared as the concentration of PAA-8 in the blend is gradually

increased. However, higher order scattering peaks appeared at a blend composition of 50% PAA by mass. A more systematic change in morphology is observed when Pluronic P105 copolymer is blended with PAA of higher molar mass (Figure 1b−d). Below a 30% PAA by mass, the morphology of Pluronic P105/PAA blends remains lamellar as ascertained from the 1:2 ratio between wave vectors corresponding to the primary and secondary scattering peaks. Additional scattering peaks appear when the blends have ≥30% PAA by mass. For example, a total of three well-pronounced higher order scattering peaks are obtained when the concentration of PAA-20 in the blend is increased to greater than 40 mass % (Figure 1b). The ratio of scattering peaks was found to be $1:\sqrt{3}:\sqrt{4}:\sqrt{7}$, which corresponds to a cylindrical morphology well ordered on a hexagonally close packed lattice. These scattering peaks were more prominent in the blend with PAA-20; however, all the samples exhibited a similar hexagonally close packed morphology albeit with more defects in the ordered lattice at a composition of 50 mass % PAA. Clearly, the addition of homopolymer increases both the effective quench depth, as observed from the disorder-to-order transition, and the volume fraction of miscible PAA/PEO− segments, $\phi_{PAA/PEO-}$.

Figure 1b also shows that extensive drying of the 30% PAA-20/Pluronic P105 blend at 80 °C under vacuum for 5 days has little effect on the final morphology. The second-order scattering peak present in the sample vacuum-dried for 24 h disappeared in the sample vacuum-dried for extended time (>120 h), but the primary scattering peak remained unchanged. While the loss of long-range order in the blend may be due to the degradation of PAA, the unaffected primary scattering peak indicates that the observed increase in effective $(\chi N)_{PEO-PPO}$ in blends is not due to the presence of residual solvent.

The effect of the homopolymer composition (mass fraction of PAA, w_{PAA}) and its molar mass (N_{PAA}) on the induced disorder-to-order transition of Pluronic P105 melts can be further assessed quantitatively from the change in character of the scattering profiles determined from the position of primary scattering peak (q^*) and its full width at half-maximum (fwhm). The position and fwhm of the primary scattering peak respectively correspond to the interdomain spacing (d-spacing) of the ordered lattice and is an indirect measure of the interfacial width of the domains. The X-ray scattering intensity was measured in arbitrary units, and thus changes in scattering intensity from different samples cannot be quantitatively compared. The position and fwhm, on the other hand, can be determined to within a 10% uncertainty by fitting the primary scattering peak to a Gaussian functional form.[49] Figures 2a,b show the change in d-spacing and fwhm as a function of copolymer mass fraction for blends. The d-spacing increased modestly but systematically ranging from 10.1 to 10.7 nm with w_{PAA-8} prior to the lamellae-to-cylindrical order−order transition. The fwhm, however, remained largely unaffected by w_{PAA} until the homopolymer concentration is increased up to 50 mass %.

A small but gradual increase in d-spacing was also observed as a function of PAA molar mass. For example, the d-spacing in blends with 20 mass % homopolymer was 10.1 nm when PAA-8 is used whereas it was 10.6 nm when PAA-88 is used instead. However, it was accompanied by a small increase in fwhm with an increase in molar mass of PAA. This peak broadening is likely due to a relative decrease in segregation strength and may be attributable to the high PAA-88 molar mass (equivalent to 96.8 kg/mol PEO) and the large entropic penalty for its mixing with the Pluronic P105 copolymer due to spatial confinement (see Discussion). On the other hand, 1-propanoic acid (AA; acrylic acid monomer) is a small molecule and has the same enthalpy for interaction with the ether oxygen of PEO via hydrogen bonding. In Figure 2c, we plot the X-ray scattering intensity measured as a function of wave vector at 80 °C for 40% PAA/Pluronic P105 blends prepared from PAA of varying molar mass. Scattering from the Pluronic P105 copolymer blended with AA at 40 mass % is uncorrelated in the observed q-range at <80 nm length scale. The lack of correlated scattering intensity suggests that the copolymer remains in a disordered state with the addition of monomeric AA. It appears that the driving force for PEO−PPO segregation in PAA/Pluronic P105 blends reaches an apparent maximum at a homopolymer molar mass between 44 and 88 kg/mol. Therefore, the increase in $(\chi N)_{PEO-PPO}$ obtained by blending PEO−PPO−PEO copolymers with PAA is due to the *polymeric* nature of the additive.

Ultrasmall-Angle X-ray Scattering. X-ray scattering from all the Pluronic P105/PAA blends exhibits a nonzero scattering intensity at low q, which is suggestive of homopolymer macrophase separation at larger length scales. A careful study of the character of this low-q scattering intensity is thus necessary to comment on the homopolymer distribution within the blend systems. We investigated the morphology of PAA/Pluronic P105 blends using ultrasmall-angle X-ray scattering (USAXS) to examine in more detail the possibility of homopolymer macrophase separation. USAXS probes the sample morphology over 4 orders of magnitude in length scale from 6 μm to 10 Å (10^{-4} Å^{-1} < q < 1 Å^{-1}) but suffers from smearing of the scattering data by the rectangular slits used to vertically collimate the incident beam. To minimize radiation damage to the sample, USAXS data were collected in logarithmically spaced scattering angles. The logarithmic spacing in q reduces the resolution of scattering peaks at high q, but the power-law scattering observed at low q is a measure of homopolymer distribution within the Pluronic P105 melt. The excess scattering intensity below $q \approx 0.01$ Å^{-1} from blends prepared at 20 mass % PAA decays similar to q^{-2} (Figure 3), which corresponds to *slit-smeared scattering* from a surface-fractal-like geometry. The presence of isolated PAA homopolymer that is macrophase-separated from the lamellar domains of the blends would have resulted in excess slit-smeared scattering intensity at low q that decays as q^{-m}, where $2 < m < 3$. Accumulation of PAA at the grain boundaries of ordered lamellae could be one reason for the surface-fractal nature of homopolymer distribution at large length scales. Excess scattering with $2 \le m \le 2.5$ was indeed observed from blends with ≥40 mass % PAA in which the cylindrical PPO microdomains are arranged on a hexagonal lattice within the matrix of miscible PAA/PEO− segments ($\phi_{PAA/PEO-} \approx 70\%$). This excess scattering is still below the Porod-type scattering ($m \approx 3$) that represents droplet macrophase separation of homopolymer.[50] We thus conclude that the homopolymer is uniformly distributed through the PEO domains of lamellae-forming blends and does not macrophase separate from the copolymer segments, regardless of its molar mass.

SCFT Simulations. The mean-field thermodynamic phase behavior of the ABA/C blend system, analogous to the PEO−PPO−PEO/PAA blend, is determined by the variables α, f_A, ϕ_c, $(\chi N)_{AB}$, $(\chi N)_{AC}$, and $(\chi N)_{BC}$ as defined in the Simulation Methods section. This is clearly a large parameter space, and identifying the specific values of parameters that dictate the phase behavior of Pluronic P105/PAA system is necessary to obtain comparison between the experimental results and simulations. However, our objective here is to simulate a blend system that is reasonably analogous to the experimental system. The volume fraction of A segments is fixed at $f_A = 0.5$; the copolymer segregation strength was fixed at $(\chi N)_{AB} = 17$, which is below the critical segregation strength required for microphase separation of neat ABA triblock copolymer. The copolymer−homopolymer segmental interaction parameters were chosen such that $(\chi N)_{AC} = -10$ and $(\chi N)_{BC} = 10$. The model does not include discrete hydrogen-bonding interactions,

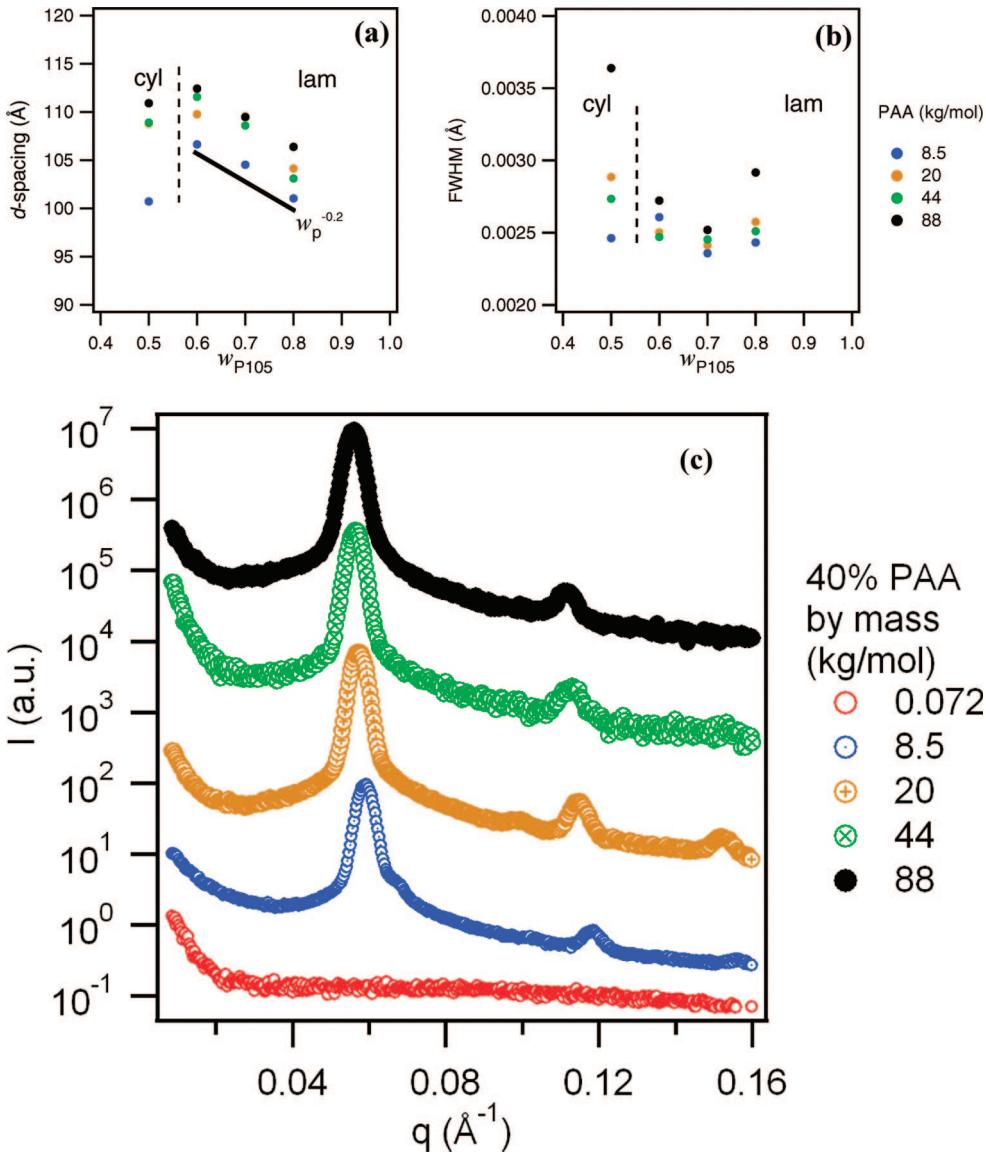

Figure 2. Change in (a) *d*-spacing and (b) full width at half-maximum of the primary scattering peak from blends discussed in Figure 1 plotted as a function of the P105 mass fraction. (c) Change in *d*-spacing with homopolymer molar mass is further supported by replotting the SAXS data in Figure 1 for blends at 40 mass % PAA.

but the parameters were chosen such that the system is qualitatively similar to a disordered triblock copolymer melt blended with a homopolymer that selectively associates with one of the (in this case A) segments.

Given these parameters, the values of ϕ_c and α were found to dramatically affect the phase behavior of the blend. Figure 4 shows the SCFT results which predict a disorder-to-order transition in a miscible copolymer melt with the addition of a homopolymer that strongly selectively interacts with one of the copolymer segments. An order−order transition from lamellar-to-cylindrical morphology occurs at $\phi_c \geq 0.2$ and is qualitatively similar to that observed in experiments. Above a homopolymer concentration ($\phi_c > 0.4$), the results predict the blend to be in a disordered state, but that may be due to the two-dimensional nature of the simulations presented here: all fields, including the segment densities, are assumed to be uniform, and the lines and holes in Figure 4 are considered infinitely long in the third (out-of-plane) dimension. The simulation framework does not accommodate spherical morphology and the miscible blend predicted at $\phi_c \approx 0.4$ may thus not necessarily represent a homogeneous state for a full three-dimensional system. The lamellar morphology in experiments is stabilized up to a blend composition of 40 mass % and is due to the presence of diblock copolymer impurity, which is not considered in simulations. Nevertheless, these results qualitatively illustrate that the increase in segregation strength achieved upon the addition of a selectively associating homopolymer. Figure 5 shows the representative blend morphologies obtained at $\phi_c = 0.1$ and 0.2 and $\alpha = 2$ and 8. The blends undergo microphase separation regardless of homopolymer chain length up to $\alpha = 8$. It is also notable that the homopolymer does not macrophase separate from the copolymer given the modest strengths of segment−segment interactions. A more quantitative evaluation of the shifts in order−disorder phase boundary with the addition of a homopolymer additive is determined using random phase approximation and will be discussed elsewhere.[51]

The interdomain spacing scaled with respect to the copolymer radius of gyration (R_g) can be obtained from the Fourier transformation of SCFT simulation results. The primary correlation peak in the structure factor profiles of blend systems is fit to a Gaussian function form to yield (*d*-spacing/R_g) data at various blend compositions.[49] Figure 6 shows the change in copolymer interdomain spacing as a function of the added homopolymer. The scaling exponent for the variation of

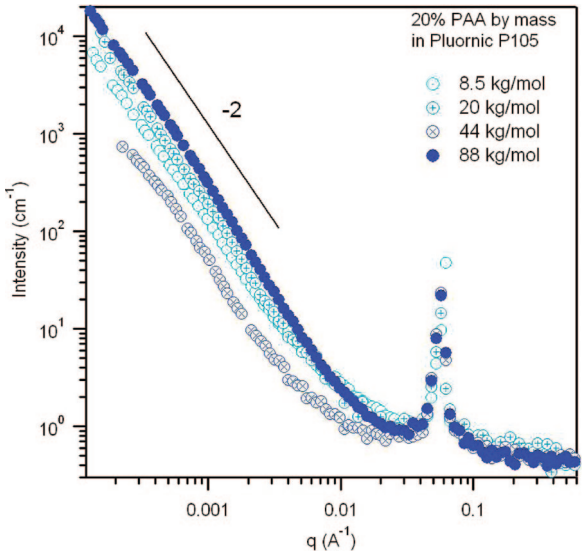

Figure 3. Rectangular slit-smeared ultrasmall-angle X-ray scattering spectra from Pluronic P105 copolymer blended with PAA at 20 mass % measured at 80 °C for homopolymers of different molar masses. The weak power law decay of scattering intensity at low q corresponds to that from surface fractals. Error in measurement of scattering intensity is smaller than the size of markers used.

d-spacing with homopolymer volume fraction obtained from SCFT simulations ($d \sim \phi_c^{-0.5}$) differs slightly from that of experiments ($d \sim w_c^{-0.2}$). The lack of a stronger dependence of the d-spacing measured in experiments may, at first, seem contrary to the arguments on selective solubilization of a homopolymer in block copolymer melts.[20,27,30] However, we use a commercially available triblock copolymer that is of moderate polydispersity ($M_w/M_n \approx 1.27$), which arises largely from PEO−PPO diblock copolymers with half the molar mass of parent triblock copolymer. The presence of such short chain diblock copolymers was shown earlier to decrease the interdomain spacing and long-range lamellar order of strongly segregated symmetric diblock copolymers.[52−54] The addition of PAA, on the contrary, is expected to increase the domain spacing and long-range order of disordered Pluronic copolymer melts.[36] The experimental results may thus be a result of the opposite effects of low molar mass diblock copolymer and selectively associating homopolymer on the lamellar interdomain spacing of Pluronic P105. The weak power-law scaling in experiments also accounts for the persistence of lamellar microphase up to a higher homopolymer loading than predicted by SCFT simulations.

Discussion

The small domain sizes achieved upon the addition of homopolymer raise an interesting question regarding the homopolymer chain conformation in these ordered blend systems. Small-angle neutron scattering measurements of blends with selectively deuterated Pluronic/PAA blend systems have earlier indicated that PAA selectively associates with PEO segments of the copolymer.[55] While this result alone may not indicate complete partitioning of PAA into PEO domains, it necessitates that the PAA segments minimize their penetration through the PPO lamellae and limit their spatial distribution to within the PEO domains.

The unperturbed radius of gyration for PAA homopolymers used can be estimated from $b(N_{PAA}/6)^{1/2}$, where b is the statistical segment length of PAA. Assuming b to be on the order of 1 nm, the unperturbed R_g for PAA homopolymers ranges from 4.4 to 14.3 nm. These dimensions may increase slightly due to the favorable enthalpy of mixing between PEO and PAA and the swelling of homopolymer as a result. The R_g of PAA-8 is the lowest among all the homopolymers studied but is similar to the domain size of PEO ($d/2 \approx 5$ nm) in blends with lamellar morphology (20 mass % PAA). The R_g of homopolymer with highest molar mass (PAA-88) is about 3−4 times that of the PEO domain size and yet is accommodated within the PEO lamellae without macrophase separation. This large mismatch between the homopolymer R_g and the size of PEO domain in ordered blends may, at first glance, suggest a significant perturbation to the homopolymer chain conformation due to confinement within two walls of soft, repulsive interactions. However, the attractive enthalpic interactions resulting from hydrogen bonding between PEO/PAA may be sufficient to offset the lower conformational entropy. All the homopolymers used in this study are relatively monodisperse, but we expect the homopolymer molar mass distribution to be an additional variable in governing the blend thermodynamics. For example, broadening the homopolymer molar mass distribution may result in an additional degree of freedom for PAA/PEO− interactions and allow for improved segregation.

The qualitative similarities between experimental results on low molar mass systems and mean-field theoretical simulations, which are strictly valid only in the high molar mass (large N) limit, merit further discussion. The neat copolymer of low molar mass used in the experiments is far from mean field, and its thermodynamic landscape is dominated by thermal fluctuations. It is known that fluctuations stabilize the disordered state of a copolymer far from the spinodal region. The formation of an ordered phase with the addition of homopolymer thus implies a suppression of fluctuations in the blend systems due probably to favorable enthalpic interaction—such as hydrogen bonding—which lowers the effective system temperature. In such a case, the mean-field approach may be more appropriate despite the low molar mass of components. The simulations also establish that disordered block copolymers of high molar mass can undergo DOT and OOT upon the addition of a selectively associating homopolymer. A more comprehensive investigation of the parametric dependency of DOT in AB/C copolymer/homopolymer blend system is beyond the scope of this study, but preliminary results from random-phase approximation analysis show that the critical ϕ_c is a complex function of the three segregation strengths $(\chi N)_{AB}$, $(\chi N)_{AC}$, and $(\chi N)_{BC}$.[54] In other words, a homopolymer with a different selective affinity toward PEO relative to that of PAA will result in a somewhat different phase map even as the molecular characteristics of block copolymer remain the same.

The Pluronic P105 triblock copolymer system examined here is laden with impurities, and yet the addition of PAA at 20 mass % was sufficient to induce a disorder-to-order transition at 80 °C. A more dramatic increase in segregation strength and a stronger dependence of d-spacing on homopolymer concentration are thus expected in the absence of impurities. While a number of copolymer/homopolymer blends were investigated in the literature,[25−30] only a few considered systems in which a selectively associating homopolymer is used.[56−60] In all the cases, however, the neat copolymer is strongly segregated and the domains undergo selective swelling with the addition of homopolymer. Recent studies of block copolymer/homopolymer blends comprising poly(vinylphenol), poly(methyl methacrylate), and poly(vinylpyrrolodine) reveal a new trend similar to the blends studied here.[61,62] The neat copolymer in that system is melt miscible, and the results suggest a homopolymer-induced microphase separation of the diblock copolymer due to the differential affinity of poly(vinylpyrrolodine) toward poly(vinylphenol). The systems, however, were only weakly ordered as observed from the lack of pronounced maximum and a rather monotonic decay of scattering intensity (Figure 9, ref 62). We are also unaware of any discussion in the literature of block

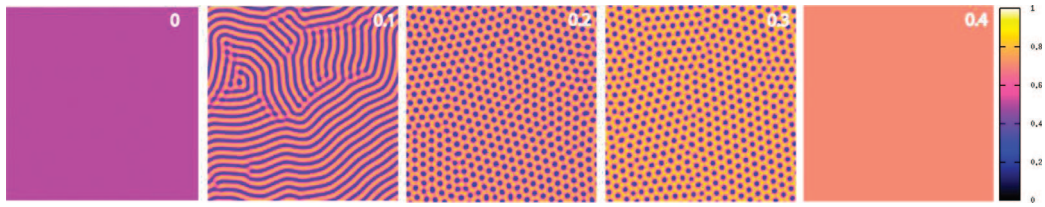

Figure 4. Self-consistent field theoretical simulations for ABA triblock copolymer of segregation strength $(\chi N)_{AB} = 17$ blended with a selectively associating homopolymer C ($\alpha = 1$) at homopolymer volume fractions shown in the legend. The thermodynamic interaction parameters of the homopolymer were chosen such that $(\chi N)_{AC} = -10$ and $(\chi N)_{BC} = 10$. The color scale to the right represents the volume fraction of miscible segments, (A + C).

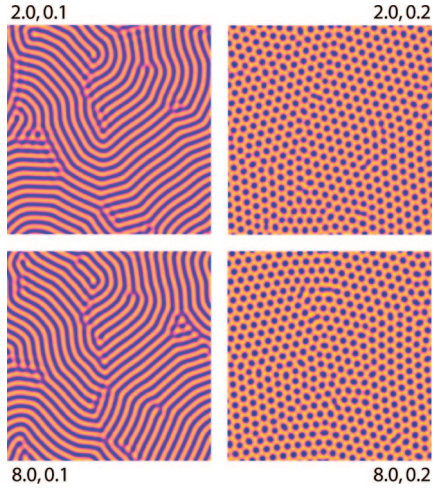

Figure 5. Self-consistent field theoretical simulations for the ABA/C triblock copolymer/homopolymer blends shown in Figure 4 but at homopolymer chain length and concentration given by the indices (α, ϕ_c) given in the legend for each result. The volume fraction of miscible (A + C) segments is represented by the color scale given in Figure 4.

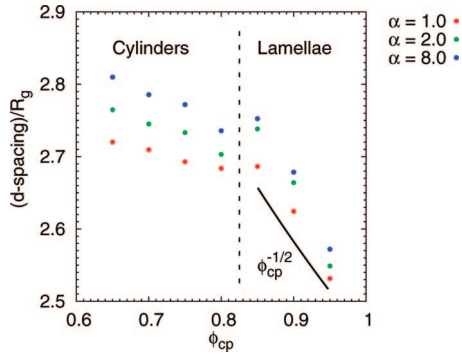

Figure 6. Scaling of interdomain spacing as a function of block copolymer volume fraction in ABA/C triblock copolymer/homopolymers blends determined from self-consistent field theory simulations at parameters discussed in Figure 4 and Figure 5. Markers correspond to the correlation length obtained from Fourier transformation of the simulation results, and the continuous line is drawn as a guide to the eye.

copolymer/homopolymer blends where the homopolymer molar mass is significantly higher than (>twice) that of the copolymer.

Conclusions

In conclusion, we show that well-ordered polymeric liquids with sub-10 nm domains can be generated by blending inexpensive low molar mass block copolymers with a homopolymer that strongly selectively associates with one of the copolymer segments via hydrogen bonding. From systematic small-angle and ultrasmall-angle X-ray scattering studies of the blend morphologies, it is established that the thermodynamics dictating the formation of ordered domains are relatively insensitive to the molar mass of homopolymer in the range 2−88 kg/mol. The formation of ordered domains maximizes the number of PEO/PAA interactions relative to that in the homogeneous state and contributes to the phenomenological origin of disorder-to-order transition in blends of Pluronic copolymers with selectively associating homopolymers. The energetic gain due to enthalpic interactions may be sufficient to overcome any entropic penalty associated with stretching the homopolymer chains even at high homopolymer molar mass. Consequently, these results allow for the use of homopolymers with a broad range of molar mass or polydispersity in practical applications.

Self-consistent field theoretical simulations provide compelling qualitative validation for the experimental microphase behavior of the weakly segregated triblock ABA/C homopolymer blend presented in this study. Specifically, the simulations show that a well-ordered, microphase-separated state can be achieved by introducing a strongly selective homopolymer to an otherwise homogeneous triblock copolymer melt. Furthermore, a lamellar to cylindrical OOT was observed with an increase in homopolymer loading. Finally, consistent with the scattering measurements, SCFT predicts a weak dependence of the microphase *d*-spacing on the hompolymer volume fraction and degree of polymerization.

This study focused on blends of commercially available inexpensive triblock copolymers blended with a commodity homopolymer. A much stronger segregation can be achieved by using a low molar mass diblock copolymer due to the lower critical χN for microphase separation of copolymers with diblock architecture relative to that of triblock. Blending with a homopolymer that enthalpically interacts with one of the copolymer segments may yet enable the facile generation of nanostructured polymeric liquids with 1−5 nm domain spacing.

Acknowledgment. This work was supported by the National Science Foundation through the Center for Hierarchical Manufacturing (CHM-NSEC) under Contracts CMMI 0531171 and CBET 0422543. Facilities supported by the NSF Materials Research Science and Engineering Center and the CHM at UMass were used in the course of this work. Use of neutron scattering facilities was supported in part by the National Science Foundation under Agreement DMR-0454672. Use of the Advanced Photon Source was supported by the U.S. Department of Energy, Office of Science, Basic Energy Sciences, under Contract DE-AC02-06CH11357. A.W.B. gratefully acknowledges support from the National Research Council Postdoctoral Research Associate program. We thank an anonymous referee for suggesting that microphase separation maximizes favorable PEO/PAA interactions and contributes to the driving force for disorder-to-order transition in blends of Pluronic copolymers with PAA.

References and Notes

(1) Yang, P. D.; Zhao, D. Y.; Margolese, D. I.; Chmelka, B. F.; Stucky, G. D. *Nature (London)* **1998**, *396*, 152–155.

(2) Templin, M.; Franck, A.; DuChesne, A.; Leist, H.; Zhang, Y. M.; Ulrich, R.; Schadler, V.; Wiesner, U. *Science* **1997**, *278*, 1795–1798.
(3) Lin, Y.; Boker, A.; He, J. B.; Sill, K.; Xiang, H. Q.; Abetz, C.; Li, X. F.; Wang, J.; Emrick, T.; Long, S.; Wang, Q.; Balazs, A.; Russell, T. P. *Nature (London)* **2005**, *434*, 55–59.
(4) Pai, R. A.; Humayun, R.; Schulberg, M. T.; Sengupta, A.; Sun, J.-N.; Watkins, J. J. *Science* **2004**, *303*, 507–510.
(5) Pai, R. A.; Watkins, J. J. *Adv. Mater.* **2006**, *18*, 241–245.
(6) Brinker, C. J.; Lu, Y. F.; Sellinger, A.; Fan, H. Y. *Adv. Mater.* **1999**, *11*, 579–585.
(7) Jenekhe, S. A.; Chen, X. L. *Science* **1999**, *283*, 372–375.
(8) Yang, P. D.; Wirnsberger, G.; Huang, H. C.; Cordero, S. R.; McGehee, M. D.; Scott, B.; Deng, T.; Whitesides, G. M.; Chmelka, B. F. *Science* **2000**, *287*, 465–467.
(9) Hamley, I. W. *Angew. Chem., Int. Ed.* **2003**, *42*, 1692–1712.
(10) Ikkala, O.; ten Brinke, G. *Chem. Commun.* **2004**, *19*, 2131–2137.
(11) Hedrick, J. L.; Miller, R. D.; Hawker, C. J.; Carter, K. R.; Volksen, W.; Yoon, D. Y.; Trollsas, M. *Adv. Mater.* **1998**, *10*, 1049–1053.
(12) Cheng, J. Y.; Mayes, A. M.; Ross, C. A. *Nat. Mater.* **2004**, *3*, 823–828.
(13) Black, C. T. *ACS Nano* **2007**, *1*, 147–150.
(14) Harrison, C.; Park, M.; Chaikin, P.; Register, R. A.; Adamson, D. H. *J. Vac. Sci. Technol. B* **1998**, *16*, 544–552.
(15) Kim, S. O.; Solak, H. H.; Stoykovich, M. P.; Ferrier, N. J.; de.Pablo, J. J.; Nealey, P. F. *Nature (London)* **2003**, *424*, 411–414.
(16) Segalman, R. A. *Mat. Sci. Eng. R* **2005**, *48*, 191–226.
(17) Bates, F. S.; Fredrickson, G. H. *Annu. Rev. Phys. Chem.* **1990**, *41*, 525–557.
(18) Bates, F. S.; Schulz, M. F.; Khandpur, A. K.; Forster, S.; Rosedale, J. H.; Almdal, K.; Mortensen, K. *Faraday Discuss.* **1994**, *98*, 7–18.
(19) Whitmore, M. D.; Noolandi, J. *Macromolecules* **1985**, *18*, 2486–2497.
(20) Matsen, M. W. *Macromolecules* **1995**, *28*, 5765–5773.
(21) Matsen, M. W. *Phys. Rev. Lett.* **1994**, *74*, 4225–4228.
(22) Vavasour, J. D.; Whitmore, M. D. *Macromolecules* **2001**, *34*, 3471–3483.
(23) Banaszak, M.; Whitmore, M. D. *Macromolecules* **1992**, *25*, 2757–2770.
(24) Likhtman, A. E.; Semenov, A. N. *Macromolecules* **1997**, *30*, 7273–7278.
(25) Winey, K. I.; Thomas, E. L.; Fetters, L. J. *Macromolecules* **1991**, *24*, 6182–6188.
(26) Tanaka, H.; Hasegawa, H.; Hashimoto, T. *Macromolecules* **1991**, *24*, 240–251.
(27) Koizumi, S.; Hasegawa, H.; Hashimoto, T. *Macromolecules* **1994**, *27*, 6532–6540.
(28) Hashimoto, T.; Tanaka, H.; Hasegawa, H. *Macromolecules* **1990**, *23*, 4378–4386.
(29) Jeon, K.-J.; Roe, R.-J. *Macromolecules* **1994**, *27*, 2439–2447.
(30) Bodycomb, J.; Yamaguchi, D.; Hashimoto, T. *Macromolecules* **2000**, *33*, 5187–5197.
(31) Ruokolainen, J.; Makinen, R.; Torkelli, M.; Makela, T.; Serimaa, R.; ten Brinke, G.; Ikkala, O. *Science* **1998**, *280*, 557–560.
(32) Ruokolainen, J.; Saariaho, M.; Ikkala, O.; ten Brinke, G.; Thomas, E. L.; Torkelli, M.; Serimaa, R. *Macromolecules* **1999**, *32*, 1152–1158.
(33) Bondzic, S.; de Wit, J.; Polushkin, E.; Schouten, A. J.; ten Brinke, G.; Ruokolainen, J.; Ikkala, O.; Dolbnya, I.; Bras, W. *Macromolecules* **2004**, *37*, 9517–9524.
(34) Epps, T. H.; Bailey, T. S.; Waletzko, R.; Bates, F. S. *Macromolecules* **2003**, *36*, 2873–2881.
(35) Epps, T. H.; Bailey, T. S.; Pham, H. D.; Bates, F. S. *Macromolecules* **2002**, *14*, 1706–1714.
(36) Tirumala, V. R.; Romang, A.; Agarwal, S.; Lin, E. K.; Watkins, J. J. *Adv. Mater.* **2008**, *20*, 1603–1608.
(37) Lee, J. H.; Balsara, N. P.; Chakraborty, A. K.; Krishnamoorti, R.; Hammouda, B. *Macromolecules* **2002**, *35*, 7748–7757.
(38) van Zoelen, W.; van Ekenstein, G. A.; Ikkala, O.; ten Brinke, G. *Macromolecules* **2006**, *39*, 6574–6579.
(39) Klymko, T.; Subbotin, A.; ten Brinke, G. *Macromolecules* **2007**, *40*, 2863–2871.
(40) Certain equipment, instruments, or materials are identified in this paper in order to adequately specify the experimental details. Such identification does not imply recommendation by the National Institute of Standards and Technology nor does it imply the materials are necessarily the best available for the purpose.
(41) Ilavsky, J.; Allen, A.; Long, G.; Jemain, P. *Rev. Sci. Instrum.* **2002**, *73*, 1660–1662.
(42) See http://usaxs.xor.aps.anl.gov/staff/ilavsky/indra_2.html.
(43) Matsen, M.; Schick, M. *Phys. Rev. Lett.* **1994**, *72*, 2660.
(44) Drolet, F.; Fredrickson, G. H. *Phys. Rev. Lett.* **1999**, *83*, 4317.
(45) Fredrickson, G. H. *The Equilibrium Theory of Inhomogeneous Polymers*; Clarendon Press: Oxford, UK, 2006.
(46) Tzeremes, G.; Rasmussen, K. O.; Lookman, T.; Saxena, A. *Phys. Rev. Lett.* **2002**, *65*, 041806.
(47) Rasmussen, K. O.; Kalosakas, G. *J. Polym. Sci., Part B: Polym. Phys.* **2002**, *40*, 1777.
(48) The uncertainty in the measurement of scattering intensity in small-angle and ultrasmall-angle X-ray scattering measurements is smaller than the markers used to denote the scattering data unless explicitly shown using error bars.
(49) The primary SAXS peak in arbitrary intensity units is fit to a Gaussian functional form to determine the peak position q^* and full width at half-maximum (fwhm). The functional form used is $I = A + B \exp[-(q - q_{peak}/2\sigma)^2]$, where A is uncorrelated scattering intensity and B is proportionality constant or intensity prefactor. $2\pi/q^*$ and σ are the reported values for d-spacing and fwhm, respectively.
(50) Porod, G. *Kolloid Z. Z. Polym.* **1951**, *124*, 83.
(51) Bosse, A. W.; Tirumala, V. R.; Lin, E. K. Manuscript in preparation.
(52) Lin, E. K.; Gast, A. P.; Shi, A.-C.; Noolandi, J.; Smith, S. D. *Macromolecules* **1996**, *29*, 5920–5925.
(53) Yamaguchi, D.; Bodycomb, J.; Koizumi, S.; Hashimoto, T. *Macromolecules* **1999**, *32*, 5884–5894.
(54) Cooke, D. M.; Shi, A.-C. *Macromolecules* **2006**, *39*, 6661–6671.
(55) Tirumala, V. R.; Vogt, B. D.; Lin, E. K.; Watkins, J. J. *Polym. Prepr.* **2006**, *47*, 757.
(56) Cohen, R. E.; Torradas, J. M. *Macromolecules* **1984**, *17*, 1101–1102.
(57) Hashimoto, T.; Kimishima, K.; Hasegawa, H. *Macromolecules* **1991**, *24*, 5704–5712.
(58) Tucker, P. S.; Barlow, J. W.; Paul, D. R. *Macromolecules* **1988**, *21*, 2794–2800.
(59) Adedeji, A.; Hudson, S. D.; Jamieson, A. M. *Polymer* **1997**, *38*, 737–741.
(60) Kim, J. R.; Hudson, S. D.; Jamieson, A. M.; Manas.Zloczower, I.; Ishida, H. *Polymer* **2000**, *41*, 9163–9168.
(61) Lee, H. F.; Kuo, S. W.; Huang, C. F.; Lu, J. S.; Chan, S. C.; Wang, C. F.; Chang, F. C. *Macromolecules* **2006**, *39*, 5458–5465.
(62) Chen, C. W.; Kuo, S. W.; Jeng, U. S.; Chang, F. C. *Macromolecules* **2008**, *41*, 1401–1410.

MA801124N